Astron. Astrophys. 270, 509–515 (1993)

ASTRONOMY AND ASTROPHYSICS

Spectral observations of active region sources with RATAN-600 and WSRT

C.E. Alissandrakis[1], G.B. Gelfreikh[2], V. N. Borovik[2], A.N. Korzhavin[3], V.M. Bogod[3], A. Nindos[1], and M.R. Kundu[4]

[1] Section of Astrophysics, Astronomy and Mechanics, Department of Physics, University of Athens, GR-15784 Athens, Greece
[2] Main Astronomical Observatory of the Russian Academy of Sciences, Pulkovo, 196140 St Petersburg, Russia
[3] St Petersburg Branch of the Special Astrophysical Observatory of the Russian Academy of Sciences, Pulkovo, 196140 St Petersburg, Russia
[4] Astronomy Department, University of Maryland, College Park Md. 20742, USA

Received August 24, accepted October 1, 1992

Abstract. We present spectral observations of neutral line and sunspot associated sources obtained with the RATAN-600 radio telescope and the WSRT in the wavelength range of 2 to 6 cm. Sources associated with large sunspots have flat spectra, while neutral line sources have very steep spectra. In the case of a large spot we estimated the magnetic field to be at least 2700 G at the base of the transition region and 1800 G in the low corona. We consider possible interpretations of the radio emission above the neutral lines. Gyroresonance emission at the fourth harmonic is inadequate, whereas emission from a small population of non-thermal electrons (total number 10^{30} to 10^{31}) with a δ=3 power law distribution seems to be sufficient.

Key words: sun: radio radiation – sun: activity – sun: sunspots

1. Introduction

High resolution microwave observations of solar active regions have shown the existence of various types of radio sources associated with sunspots, plages, coronal loops and regions of transverse magnetic fields or neutral lines.

The sunspot component (Gelfreikh & Korzhavin 1976; Kundu et al. 1977; Akhmedov et al. 1988) is bright with a brightness temperature of 0.5-2.5 10^6 K, in some cases up to 4-5 10^6 K; it has a fairly simple structure in total intensity, covering an area of about the size of the sunspot or smaller, sometimes with a depression above the umbra (Alissandrakis & Kundu 1982, 1984). The circular polarization is higher at the edge of the total intensity source, forming a "ring" or "horseshoe" structure (Alissandrakis & Kundu 1982; Lang & Willson 1982; Strong et al. 1984; Akhmedov et al. 1990). Model computations (Gelfreikh & Lubyshev 1979; Alissandrakis et al. 1980; Alissandrakis 1980) have confirmed that the primary emission mechanism is gyroresonance (g-r) emission from the low harmonics of the gyrofrequency (Zheleznykov 1962; Kakinuma & Swarup 1962). The structure of the source depends upon which of the low order (first to fourth) harmonics of the gyrofrequency are located in regions of high temperature, i.e. the transition region (TR) or low corona.

The plage associated sources are weaker ($T_b \sim 10^5$ K at cm wavelengths) and their emission is usually attributed to the free-free process (e.g. Kundu et al. 1977) but there is some evidence of non-thermal emission from observations in the range of 20-30 cm (Gelfreikh et al. 1990). The halo component is associated with the active region as a whole and is dominated in the range of 10-20 cm ($T_b \sim$ 2 to 5 10^6 K). Their emission mechanism is most probably gyrosynchrotron emission from non-thermal electrons with a power-law distribution (Akhmedov et al. 1987). Some fine loop-like structures are observed in this wavelength range, but their contribution to the total flux of the active region is less than 5 per cent (Akhmedov et al. 1986, 1987).

The strongest component observed in active regions at cm wavelengths is associated with neutral lines (Kundu & Alissandrakis 1984; Akhmedov et al. 1986, 1987; Alissandrakis et al. 1992). In the range of 2-4 cm this component, called "the peculiar source", is observed only in proton flare producing active regions. The peculiar sources are characterized by some unique features (Akhmedov et al. 1989; Borovik et al. 1989a, 1989b, 1989c). These compact radio sources dominate in intensity over all the other components of active region emission at short centimeter wavelengths. They have a moderate (5-30 %) degree of circular polarization. Their positions are related to neutral lines of the photospheric magnetic field in the region of its steepest gradient or near intrusions of opposite magnetic flux. An important characteristic of peculiar sources is their high brightness temperature (7-8 10^6 K at 3-4 cm) and extremely steep flux spectra at the shortest wavelengths. The lifetime of these sources is several days and they are stable even after flares. The emission mechanism of the peculiar sources is still an open question since it is not clear whether the dominant emission mechanism is gyroresonance emission, or gyrosynchrotron emission (from

Send offprint requests to: C.E. Alissandrakis

non-thermal particles or from very hot thermal plasma), or even the f-f process (Vatrushin & Korzhavin 1989; Korzhavin et al. 1989).

Strong neutral line associated sources were observed at 6.16 cm with the WSRT in large, complex active regions (Alissandrakis & Kundu 1982; Kundu & Alissandrakis 1984). Simultaneous X-ray observations showed that they corresponded to arcades of x-ray loops. The high brightness temperature at 6.16 cm of these sources could not be interpreted in terms of thermal free-free emission (Strong et al. 1984).

In this paper we present flux spectra of these sources, together with spectra of sunspot associated sources, from simultaneous WSRT and RATAN-600 observations. The WSRT and RATAN-600 data complement each other. The WSRT provides high angular resolution in two dimensions but only at one wavelength, while the RATAN-600 provides nearly simultaneous one-dimensional scans at five wavelengths close enough to determine the flux spectra of the active region sources. On the other hand the confusion arising because of the poor angular resolution of the RATAN-600 can be compensated in part by the WSRT observations.

2. Observations and data processing

The WSRT observations were obtained at 6.16 cm (4874 MHz, bandwidth 10 MHz) from May 22 to 27, 1980. Approximately 12 hours of observations were used daily to produce synthesis maps of Hale regions 16862, 16863 and 16864 in total intensity (I) and circular polarization (V), with an E-W resolution of 3.6″-4.2″ and a N-S resolution of 10.0″-12.2″. The observing procedure and the data reduction process has been described by Kundu & Alissandrakis (1984).

The radio telescope RATAN-600 was used as a combination of the south sector of the main reflector, the flat periscopic mirror and the secondary parabolic mirror (Akhmedov et al. 1987; Andrianov et al. 1990). The solar radio emission was observed daily during the Sun's transit through the local meridian. Both total intensity and circular polarization were recorded simultaneously at five wavelengths: 2.0, 2.3, 2.7, 3.2, and 4.0 cm (circular polarization measurements at 2.7 cm were recorded only in analog form). The HPBW of the RATAN-600 (in the E-W and the N-S directions) was 17″ by 13′, 19″ by 15′, 23″ by 18′, 27″ by 21′ and 34″ by 26′ respectively. Antenna temperatures were corrected for aberration losses due to shifting of the feed out of focus and for the dependence of the effective antenna area on the wavelength.

We used two methods for the measurement of the source flux from the RATAN scans. In the first method the flux was measured on plots of the one dimensional flux vs position and the sources as well as the quiet sun background were estimated by visual inspection. In the second, the quiet Sun emission was computed by performing successive parabolic fits of the digital data; in each iteration only points with intensity less or equal to the corresponding values of the previous parabolic fit were taken into account. When no more data points were rejected, the computed quiet Sun emission was subtracted from the RATAN-600

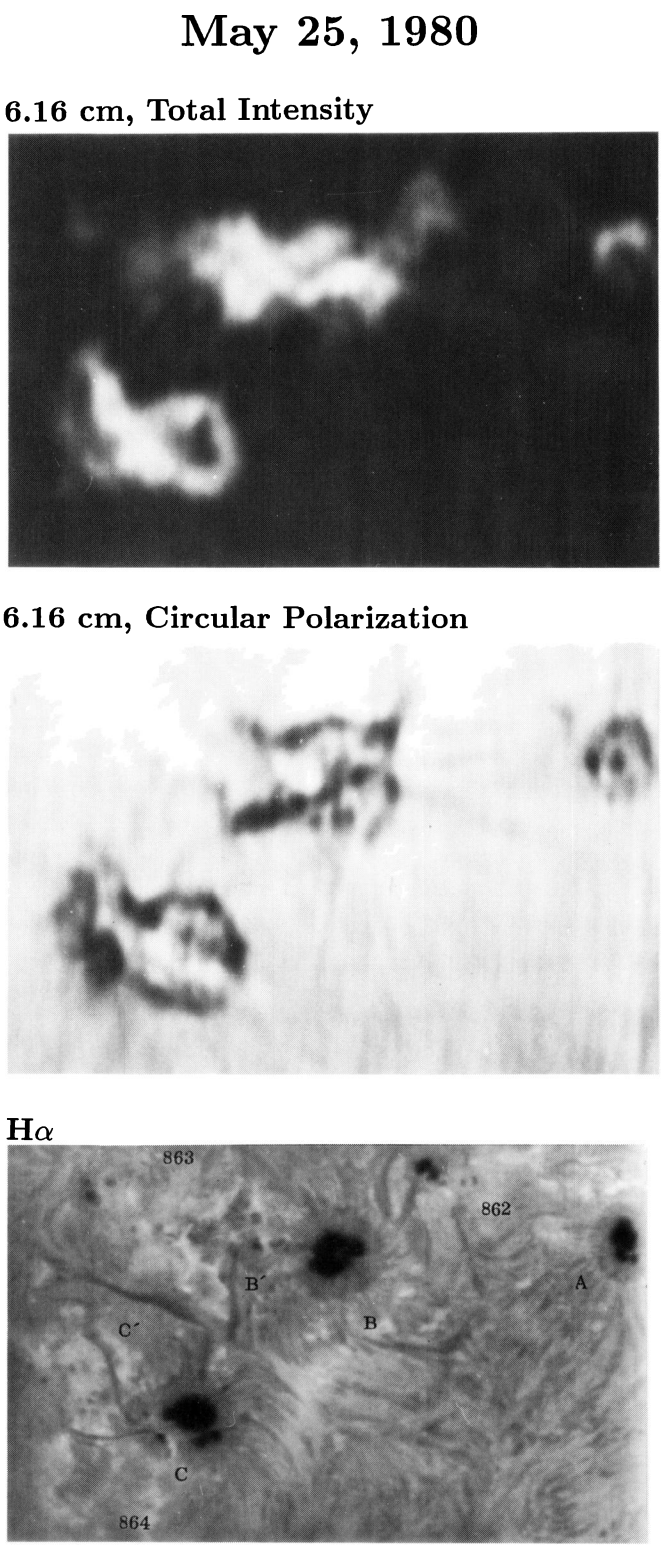

Fig. 1. Photographic representations of WSRT I and V maps at 6.16 cm, together with an Hα photograph (National Observatory of Athens), on May 25, 1980. The field of view of the WSRT images is 420″ by 280″. Celestial North is up, celestial West to the right. Left hand circular polarization is dark

scans. Subsequently, the flux of each local source was computed by modeling the data to gaussian-shaped sources. The two methods gave consistent results, within about 10%. We computed flux spectra for I, V, R (right circularly polarized intensity) and L (left-hand circularly polarized intensity). An interpolation was used for the flux densities at 2.7 cm in R, L and V due to the lack of digital V data. The 6 cm flux was computed directly from the 2-dimensional maps, where the sources were separated by visual inspection.

Results from the data obtained during May 22-27 with the WSRT have already been reported by Alissandrakis & Kundu (1982), Strong et al. (1984), Alissandrakis & Kundu (1984), Kundu & Alissandrakis (1984). In this paper we take advantage of the spectral information provided by the combined RATAN-WSRT data, to study the three-dimensional structure of active region sources and to discuss some open questions such as the emission mechanism of neutral-line-associated sources; we also discus the origin of the ring source in Hale region 16864.

3. Results

We selected May 25 for a detailed study, because observations at all six wavelengths were available on this day and also because the active regions were located near the central meridian. Figure 1 shows the I and V WSRT maps for May 25, together with an Hα photograph from the Observatory of Athens (see Alissandrakis & Kundu 1982; Kundu & Alissandrakis 1984, for a detailed discussion of the various radio features and a comparison with chromospheric and magnetic field structures). We would like to point out that practically all polarized emission was in the left circular sense, which corresponds to the extraordinary mode in regions of negative polarity (leading part of the active regions); this is due to polarization inversion in the trailing part of the regions, as a result of Q-T wave propagation. However, the polarization inversion lines were located well to the east of the neutral line sources and they did not influence our measurements of the total V flux.

The most prominent radio sources of the active region complex are labeled A, A', B, B', C and C'. Sources A and A' are associated with the leading and trailing spots respectively of the active region 16862. Sources B and C are associated with the big spots of active regions 16863 and 16864, while sources B' and C' are associated with the main neutral lines of active regions 16863 and 16864 respectively.

The RATAN-600 I scans at 2.0, 2.3, 2.7, 3.2 and 4.0 cm and the V scans at 2.0, 2.3, 3.2 and 4.0 cm for the same day are shown in Fig. 2. For the sake of comparison, we give in the same figure the WSRT data integrated along the N-S direction and degraded to the resolution of the RATAN 2 cm scan. The corresponding R and L scans are given in Fig. 3.

All sunspot associated sources are already visible at 2 cm (Fig. 2). At this wavelength they are strongly polarized, with little or no emission in the o-mode (R polarization, Fig. 3). For g-r emission, the absence of o-mode emission is an indication that only one harmonic of the gyrofrequency (presumably the third) is located above the chromosphere. As a general trend,

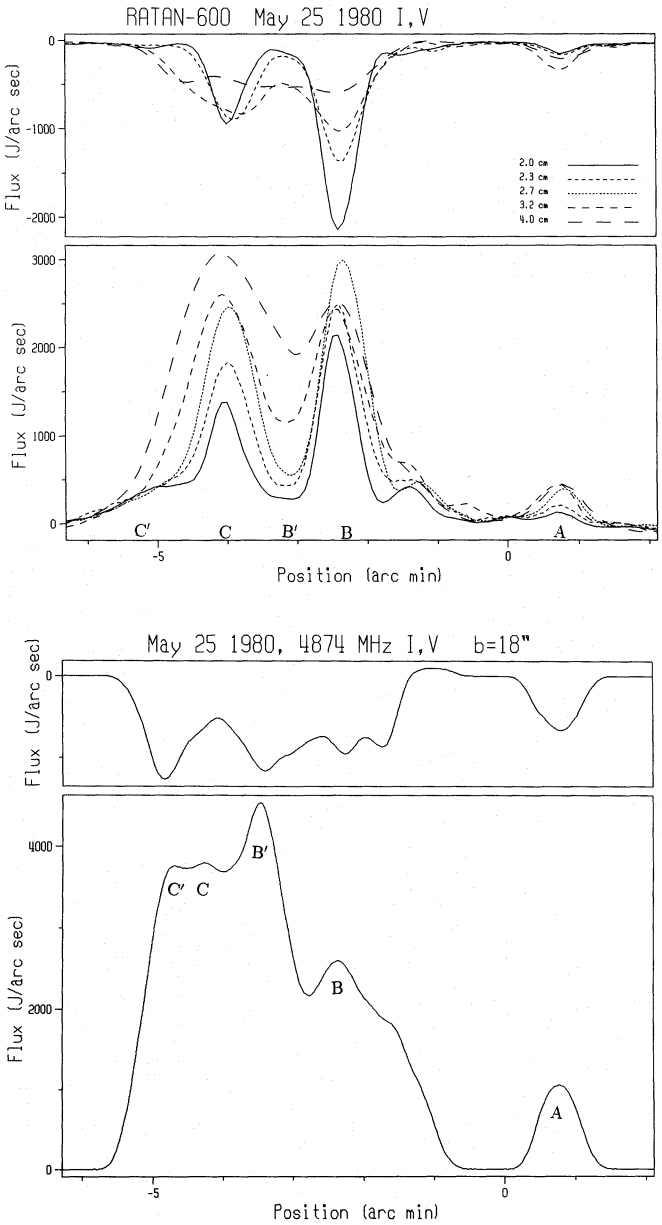

Fig. 2. One dimensional scans of the active region complex obtained with the RATAN in I and V, together with the WSRT data integrated along the N-S direction and convolved with the RATAN 2 cm beam

the total intensity increases and the polarization decreases with wavelength, a reflection of the fact that the harmonic layers move higher, into hotter regions of the TR and, at the same time, their opacity increases.

An inspection of the I, R and L scans from 2 to 2.7 cm reveals that emission peaks shifted progressively from the east (limbward) side of the spot towards the center as the wavelength increased. This is a direct consequence of the fact that the g-r opacity is higher at the limbward side of the spot, where the angle between the magnetic field and the line of sight is also higher. Hence, at short wavelengths the emission has the form of a crescent, located above the limbward side of the spot; as

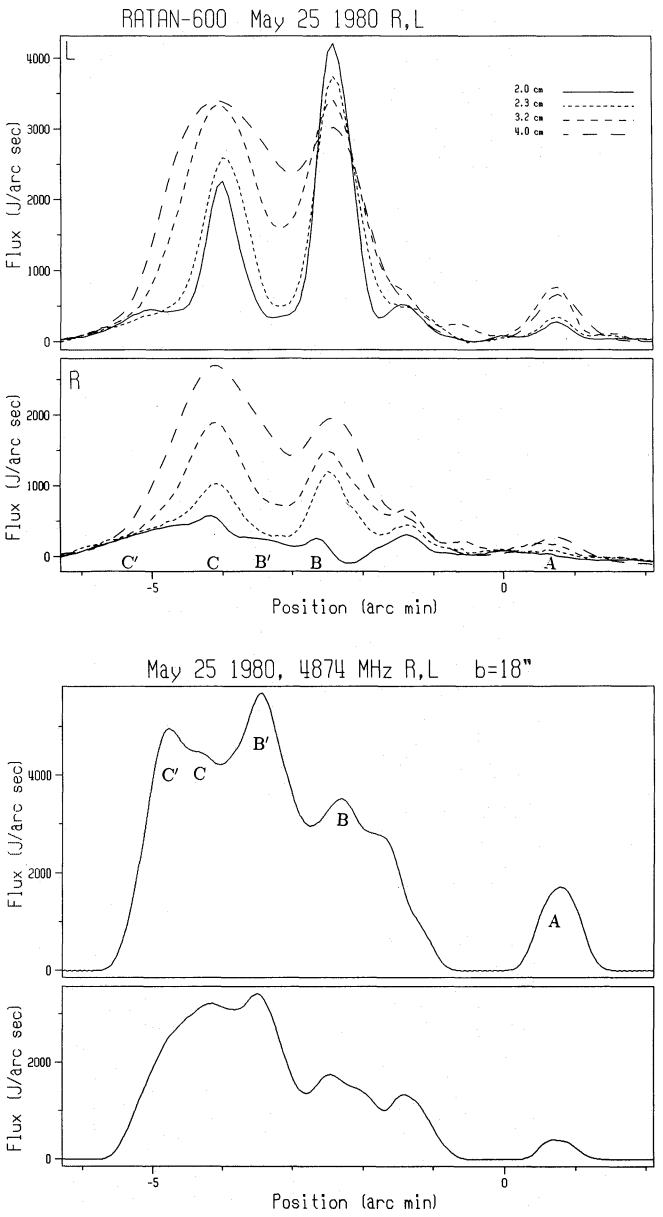

Fig. 3. Same as Fig. 2 for right and left hand circularly polarized emission

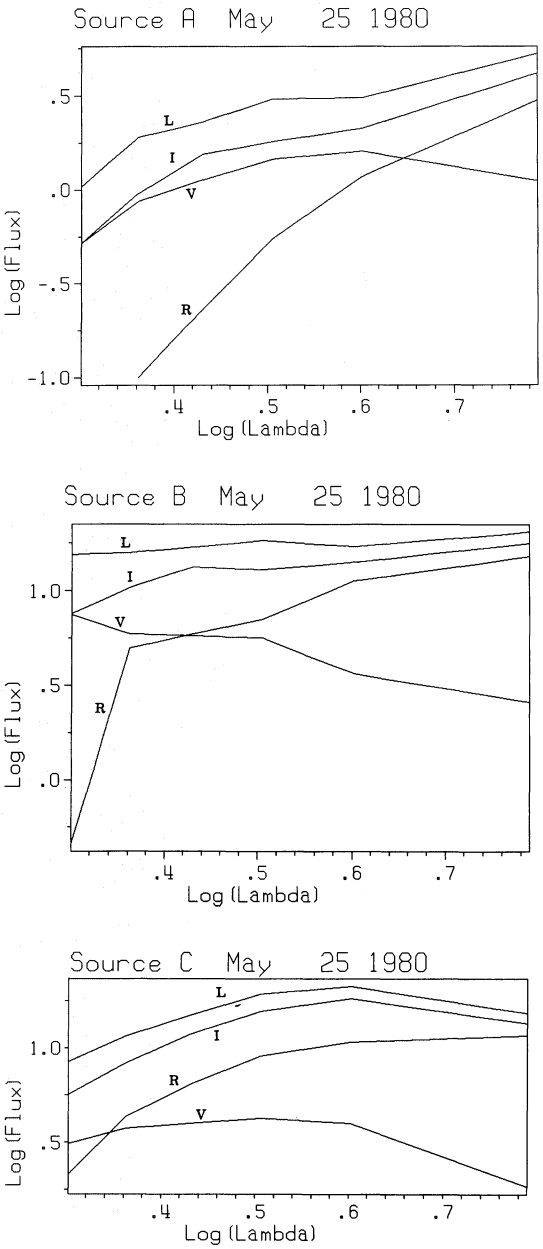

Fig. 4. Flux spectra (in sfu) of the sunspot associated sources A, B, C

the opacity increases with wavelength, the size of the emission region increases and its center of gravity shifts towards the center of the spot.

The neutral line sources are practically invisible at short wavelengths. At 3.2 cm they are clearly visible as intensity enhancements, east of the sunspot associated sources B and C, whereas at 6.16 cm they dominate the integrated scans.

4. Flux spectra

4.1. Sunspot associated sources

Figure 4 gives the flux spectra in total intensity and circular polarization, as well as in right and left hand polarized intensity for the sunspot associated sources A, B and C. Before discussing these results, we would like to remind the reader of the flux spectra predicted by the g-r theory. Emission in the e-mode comes primarily from the third or lower harmonics of the gyrofrequency, whereas o-mode emission comes from the second harmonic. As the wavelength increases, a given harmonic layer moves higher, in hotter regions of the atmosphere where the magnetic field strength is lower. At very short wavelengths there is no emission because even the third harmonic is below the TR. As the wavelength increases the third harmonic enters the TR, which gives high e-mode emission and practically no o-mode emission; hence the source is almost 100% polarized. The e-mode emission increases with wavelength until the harmonics

rise in the upper part of the TR where the temperature gradient is small and cannot compensate the effect of the λ^2 factor; after that the flux decreases, due to the λ^2 factor. The o-mode has a similar spectrum, shifted to longer wavelengths. As the second harmonic enters the TR, the o-mode emission increases sharply and the circular polarization decreases.

Let us now go back to the observed spectra. Source A is associated with a moderate size spot, with a photospheric magnetic field strength of about 2500 G (according to Solar Geophysical Data). The form of the source at 6.16 cm shows that both the second and third harmonics are responsible for the emission at that wavelength (Alissandrakis & Kundu 1984). The I and L (e-mode) flux increased in the entire range of 2 to 6.16 cm, whereas the V flux peaked at 4 cm. There is significant e-mode emission at 2 cm, but practically no o-mode emission up to at least 2.3 cm (cf. Fig. 3). This shows that at 2 cm the third harmonic was already in the TR, whereas the second harmonic entered the TR at wavelengths longer than 2.3 cm. Combining these results, we get a lower limit of 1800 G and an upper limit of 2350 G for the strength of the magnetic field at the base of the transition region. In the upper TR/low corona, Alissandrakis and Kundu estimated the strength of the magnetic filed to be in the range of 600 to 900 Gauss.

The flux spectrum of source B differs from that of source A in that the L and I spectra are nearly flat while the V spectrum decreases with wavelength above 2 cm. Such extended flat spectra have been predicted by model computations (Krüger et al. 1985). This form of spectrum indicates that, at 2 cm, the second harmonic is not simply inside the TR, but well into the low corona. At the same time the ordinary emission at 2 cm is weak, therefore the second harmonic is apparently located in the low transition region. The implication is a magnetic field strength of at least 2700 G at the base of the transition region and at least 1800 G at the base of the corona. These values are much higher than for source A, which is not surprising since source B is associated with a much bigger spot with a photospheric field of 3000 G.

Sunspot-associated source C is of particular interest because it had a ring structure at 6 cm, i.e. a brightness temperature depression at about the middle of the umbra (Alissandrakis & Kundu 1982; Strong et al. 1984). Soft X-ray data were used to derive the electron temperature and density of the coronal material of the ring structure (Strong et al. 1984; Siarkowski et al. 1989). However, contradictory results have been reported: Strong et al. found no significant depression in electron temperature above the umbra, while Siarkowski et al. did find a depression of 0.7 10^6 K. From the radio point of view, however, the only possible interpretation is in terms of the presence of low temperature material above the spot umbra (cf. Foukal et al. 1974) or even as a rather abnormal increase of temperature above the penumbra.

The flux spectrum of source C is intermediate between those of sources A and B; it is not as flat as B and not as steep as A, moreover the I and L spectra peak at 4 cm and the V spectrum peaks at 3.2 cm. In terms of magnetic field, these results imply

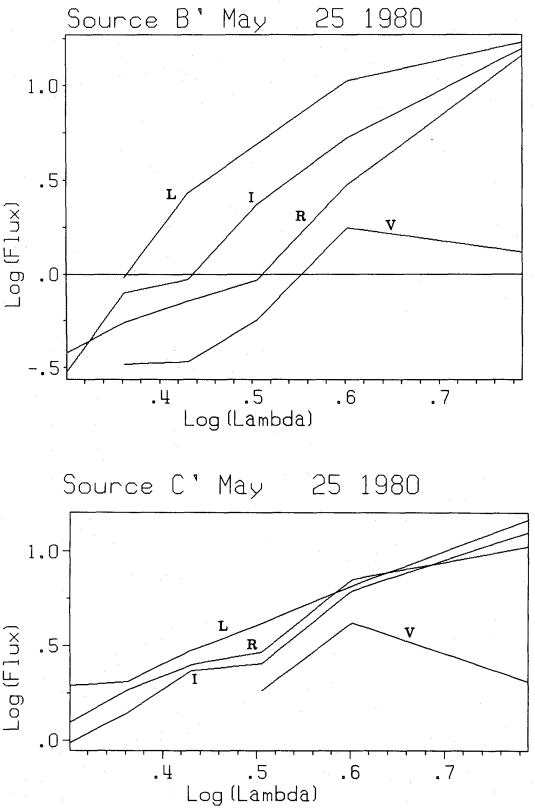

Fig. 5. Flux spectra of the neutral line sources B' and C'

strengths somewhat lower than for source B, of the order of 1800 G in the upper TR and 2700 G in the low TR.

An interesting question is whether the low temperature region is also detectable at lower wavelengths. Unfortunately the one-dimensional scans provide no evidence; this is apparently due to the combined effects of integration and lower resolution, since neither the integrated 6.16 cm data show any trace of the ring structure. However, the smooth variation of the flux indicates that there is probably no drastic change of source structure with wavelength.

4.2. Neutral line associated sources

The neutral line sources B' and C' were located in regions of high magnetic field gradient and were associated with arch filament systems at least for part of our observing period (Kundu & Alissandrakis 1984). Strong et al. 1984 detected X-ray sources, presumably arcades of loops, at the same location.

The present observations show that neutral line sources are characterized by an exceptionally rapid increase of flux density with wavelength (Fig. 5), compared to the flux spectra of sunspot-associated sources (Fig. 6). Comparing the spectral, geometrical and temporal characteristics of sources B' and C' with the same data of peculiar sources (Korzhavin et al. 1989) we conclude that they are very similar; they differ in that their spectra are displaced to longer wavelengths and the sources are associated with active regions of moderate activity (no proton

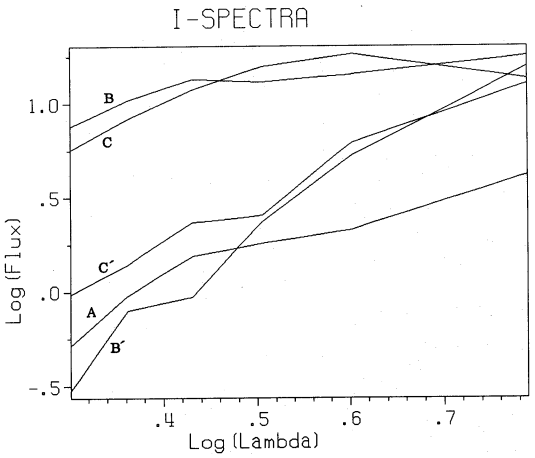

Fig. 6. Flux spectra of all sources in total intensity

flare occurred). It appears that both types of neutral line sources are of the same nature, with some quantitative difference (i. e. weaker magnetic field). In any case, these sources are located in coronal regions where continuous energy release might occur, probably from stable current sheets.

We shall now investigate the possible emission mechanisms of sources B' and C'. The fast increase of flux with wavelength rules out the f-f process. The same conclusion was reached by Strong, Alissandrakis & Kundu 1984, who determined the density and the temperature from soft X-ray data and found that the f-f optical depth and the corresponding brightness temperature of the sources was much lower than that observed at 6 cm.

A possible interpretation might be in terms of g-r emission from harmonics higher than the third; indeed, above the neutral line, the angle between the magnetic field and the line of sight is large and the absorption coefficient increases by several orders of magnitude compared to that at small angles. The magnetic field required to give resonance for the fourth harmonic at 6.16 cm is 430 Gauss. Using that value, together with $\theta \sim 85°$, $L \sim 10^9$ cm, $N_e = 7.3\,10^9$ cm^{-3}, $T_e = 3\,10^6$ K for source B' and $N_e = 4.6\,10^9$ cm^{-3}, $T_e = 3.3\,10^6$ K for source C' (values given by Strong et al. 1984), we found that the g-r optical depth was $\sim$1.4 for the e-mode and $\sim$0.2 for the o-mode and the brightness temperature $1.5\,10^6$ K and $0.9\,10^6$ K for I and V respectively. These values cannot account for the low degree of circular polarization observed at 6 cm; in addition they cannot reproduce the observed brightness temperatures of the sources ($> 2.75\,10^6$ K). In order for the fourth harmonic to be optically thick in both the e-mode and the o-mode we need implausibly high electron densities (10^{11} cm^{-3}). Further evidence against the g-r process is that the value of the magnetic field required for fourth harmonic emission is probably too high for regions above magnetic field neutral lines, where weaker fields are expected to prevail.

The steep spectra of the neutral line sources may imply that the emission mechanism is gyrosynchrotron radiation from mildly relativistic electrons. This assumption was checked against the computations made by Chiuderi-Drago & Melozzi (1984). In order to better compare our results to their model we transformed their computed spectra of brightness temperature to flux density spectra using the FWHM of the corresponding gaussian-shaped model sources and assuming circular symmetry.

The short wavelength part (2-2.7 cm) of the spectra of the sources was not steep and may be interpreted in terms of emission from nearby pores. The slope of the I spectra from 3.2 to 6 cm can be used to estimate the power law index δ of the non-thermal particles, under the synchrotron approximation. We found δ=3.3 and δ=2.5 for sources B' and C' respectively and we used δ=3 in our further computations. Once the value of δ is known, the computation of Chiuderi-Drago & Melozzi (1984), together with the observed value of the degree of circular polarization, can be used to estimate the strength and direction of the magnetic field. The observed values at 3.2 and 4 cm were reproduced assuming $\theta = 70°$ and a magnetic field of 150 G for source B' and 200 G for source C'. However, the above value of θ did not fit the low degree of circular polarization at 6 cm ($\sim$10%); a value of $\theta \sim 85°$ seemed to be more appropriate for 6 cm.

The values of the magnetic field and the angle between the magnetic field and the line of sight were used to derive the emission coefficient, again from the computations of Chiuderi-Drago & Melozzi (1984). Once the emission coefficient is computed, the calculation of flux density spectra is straightforward, provided that the coronal plasma is optically thin. We reproduced the observed flux density spectra assuming typical values of the total number of electrons in the range $3.5\,10^{30}$ to 10^{31}.

5. Conclusions

Our observations confirmed the well-known fact that g-r process is the main emission mechanism of sunspot-associated sources. Their emission was characterized by features predicted from model computations. At short wavelengths, e-mode and o-mode emission peaks were located at the limbward side of sunspots and moved progressively towards the center as the wavelength increased. Flux spectra of sources associated with big sunspots were flatter, compared to those associated with a smaller spot. This effect is due to the dependence of the g-r process on the magnetic field: the stronger the magnetic field the shorter is the wavelength for which a given harmonic rises into the transition region. Consequently the flat spectra of these sources can be explained as due to the presence of both the second and third harmonics in the upper TR or low corona, even at the shortest wavelength observed. Of course, a steep spectrum would be expected at wavelengths even shorter than 2 cm.

Once the harmonics responsible for the emission have been identified, they provide a straight forward estimate of the magnetic field. We thus estimated field strengths as high as 2700 G at the base of the transition region and as high as 1800 G in the low corona for spots with a photospheric magnetic field of 3000 G (Table 1). Akhmedov et al. 1982, using RATAN-600 data, measured field strengths between 1420 and 2200 G at the base of the transition region, while White et al. (1991) measured 1800 G at

Table 1. Magnetic field strength above sunspots

Hale region	Low TR (Gauss)	Upper TR/Low Corona (Gauss)
16862	1800-2350	600-900
16863	>2700	>1800
16864	~2700	~1800

the level of 6.4 10^5 K from VLA data at 2 cm. Thus the present measurements are among the highest values ever reported.

The high values of magnetic field strength indicate that the base of the TR is located fairly low above spots or, equivalently, a more efficient heating there. The requirement of additional energy supply above sunspots to make their g-r emission at short wavelengths (like 3 cm) possible was already pointed out by Livshits et al. (1966). The extra heating may be due to additional flux of MHD waves, carried from under the photosphere into the magnetic flux tube of the spot.

The brightening at the edge of sunspot associated source *C* at 6 cm implies a higher electron temperature of the corona above the penumbra. We propose that this may be due to the inhomegeneous structure of this region (known also from optical observations). Indeed, it is worth noting that the bright source observed by White et al. (1991) at 2 cm was located above the penumbra of a sunspot. The fine structure may cause (or demonstrate) the process of coupling and conversion of different types of MHD waves and consequently their dissipation.

Finally we investigated the flux spectra and the emission mechanism of neutral line associated sources. The spectra are much steeper than those of sunspot associated sources and very similar to those of peculiar sources observed at shorter wavelengths (Akhmedov et al. 1986). Our computations ruled out both the f-f process and the gyroresonance mechanism from the fourth or lower harmonics. The former was ruled out due to the observed steep spectra while the latter due to the extremely high electron densities (~10^{11} cm^{-3}) required to make the fourth harmonic optically thick in both the e-and the o-mode. It is possible that the emission mechanism is gyrosynchrotron radiation from mildly relativistic electrons with a power law index of the order of 3. Assuming magnetic fields of 150-200 G, high values of the angle between the magnetic field and the line of sight (70° - 85°) and an emitting volume containing about 10^{30} - 10^{31} non-thermal particles, we can successfully reproduc the observable quantities of neutral line sources.

Acknowledgements. This work has been supported in part through the bilatteral exchange agreement between Greece and the USSR. This research at the University of Maryland was supported by NSF grant ATM 90-19893 and NASA grant NAG W-1541 The WSRT is operated by the Netherlands Foundation for Radio Astronomy with financial support from the Netherlands Organization for the advancement of Pure Research (ZWO).

Akhmedov Sh. B., Gelfreikh G. B., Bogod V. M., Korzhavin A. N., 1982, Solar Phys., 79, 41
Akhmedov Sh. B., Borovik V. N., Gelfreikh G. B., Bogod V. M., Korzhavin A. N., Petrov Z. E., Dikij V. N., Lang K. R., Willson R. F., 1986a, ApJ, 301, 460
Akhmedov Sh. B., Bogod V. M., Gelfreikh G. B., Hildebrandt J., Krüger A., 1986b, Contr. Astr. Obs. Skanlante Pleso, 15, 339
Akhmedov Sh. B., Bogod V. M., Borovik V. N., Willson R. F., Gelfreikh G. B., Dikij V. N., Korzhavin A. N., Lang K. R., Petrov Z. E., 1987, Astrofiz. Issled. (Izv. SAO), 25, 105
Akhmedov Sh. B., Bogod V. M., Borovik V. N., Gelfreikh G. B., Dikij V. N., Korzhavin A. N., Shatilov V. A., 1988, in Solar Maximum Analysis, Proceedings of the SMA Workshop, Irkutsk, USSR, Nauka, Novosibirsk, 1988, p. 76
Akhmedov Sh. B., Borovik V. N., Gelfreikh G. B., Bogod V. M., Korzhavin A. N., Petrov Z. E., Hofmann A., Bahmann G., 1989, Astrofiz. issled. (Izv. SAO), 28, 111
Akhmedov Sh. B., Bogod V. M., Korzhavin A. N., Aurass H., Hildebrandt J., Krüger A. 1990, Solar Phys., 129, 351
Andrianov S. A., Akhmedov Sh. B., Bogod V. M., Boldyrev S. I., Borovik V. N., Gelfreikh G. B., Zueva V. A., Korzhavin A. N., Petrov Z. E., Plotnikov V. M., Plotnikova G. B., Chekh S. A., 1990, Solar Radio Observations with the RATAN-600 Radiotelescope in the Wavelength Range of 2-4 cm During the Period of the Solar Maximum Year, Moscow
Alissandrakis C. E., 1980, in Radio Physics of the Sun, eds M. R. Kundu, T. Gergely, Reidel, Dordrecht, p. 101
Alissandrakis C. E., Kundu M. R., 1982, ApJ, 253, L49
Alissandrakis C. E., Kundu M. R., 1984, A&A, 139, 271
Alissandrakis C. E., Kundu M. R., Lantos P., 1980, A&A, 82, 30
Alissandrakis C. E., Lubyshev, B. I., Smolkov G. Ya., Krissinel B. B., Treskov T. A., Miller V. G., Kardapolova N. N., 1992, Solar Phys., *in press*
Borovik V. N., Drake N. A., Golovko A. A., 1989a, in Solar Magnetic Fields and Corona, Nauka, Novosibirsk, v. 2, p. 162
Borovik V. N., Vatrushin S. M., Korzhavin A. N., 1989b, Astrofiz. Issled. (Izv. SAO), 28, 123
Borovik V. N., Drake N. A., Korzhavin A. N ., Plotnikov V. M., 1989c, Kin. Fiz. Neb. Tel, Kiev, 5, 63
Chiuderi-Drago F., Melozzi M., 1984, A&A, 131, 103
Gelfreikh G. B., Lubishev B., 1979, AZh, 56, 562 (SvA, 23, 316)
Gelfreikh G. B., Ipatova L. P., Korzhavin A. N., Shatilov V. A., 1990, Astrofiz. Issled. (Izv. SAO), 29, 3
Gelfreikh G. B., Korzhavin A. N. 1976, in Fizika Solnechnykh Pyaten, Irkutsk, p. 94
Kakinuma T. M., Swarup G., 1962, ApJ, 136, 975
Korzhavin A. N., Gelfreikh G. B., Vatrushin S. M., 1989, in Solar Magnetic Fields in the Corona, Nauka, Novosibirsk, v. 2, p. 119
Kundu M. R., Alissandrakis C. E., Bregman J. D., Hin A. C., 1977, ApJ, 213, 278
Kundu M. R., Alissandrakis C. E., 1984, Solar Phys., 94, 249
Krüger A.,Hildebrandt J., Furstenberg F., 1985, A&A, 143, 72
Lang K. R., Willson R. F., 1982, ApJ, 255 L111
Livshits M. A., Obridko V. N., Pikelner S. B., AZh, 43, 6 (SvA, 10, 6)
Siarkovski M., Sylwester J., Jakimiek J., Bently R. D., 1989, Solar Phys., 119, 189
Strong K. T., Alissandrakis C. E., Kundu M. R., 1984, ApJ, 277, 865
Vatrushin S. M., Korzhavin A. N., 1989, in Fizika Solnechnoy Plazmy, Nauka, Moscow, p. 100
White S. M., Kundu M. R., Gopalswamy N., 1991, ApJ, 366, L43
Zheleznyakov V. V., 1962, AZh, 39, 5 (SvA, 6, 3)
Zheleznyakov V. V., 1970, Radio Emission of the Sun and Planets, Oxford, Pergamon Press